



HAL
open science

A local statistic for the spatial extent of extreme threshold exceedances

Ryan Cotsakis, Elena Di Bernardino, Thomas Opitz

► **To cite this version:**

Ryan Cotsakis, Elena Di Bernardino, Thomas Opitz. A local statistic for the spatial extent of extreme threshold exceedances. 2023. hal-04246931

HAL Id: hal-04246931

<https://hal.science/hal-04246931>

Preprint submitted on 17 Oct 2023

HAL is a multi-disciplinary open access archive for the deposit and dissemination of scientific research documents, whether they are published or not. The documents may come from teaching and research institutions in France or abroad, or from public or private research centers.

L'archive ouverte pluridisciplinaire **HAL**, est destinée au dépôt et à la diffusion de documents scientifiques de niveau recherche, publiés ou non, émanant des établissements d'enseignement et de recherche français ou étrangers, des laboratoires publics ou privés.

A local statistic for the spatial extent of extreme threshold exceedances

Ryan Cotsakis^{1,a,*} Elena Di Bernardino^{1,b} Thomas Opitz^{2,c}

¹Université Côte d'Azur, Laboratoire J.A. Dieudonné, UMR CNRS 7351, Nice, France.

^aRyan.Cotsakis@univ-cotedazur.fr, ^bElena.Di.Bernardino@univ-cotedazur.fr

²Biostatistics and Spatial Processes, INRAE, Avignon, France; ^cThomas.Opitz@inrae.fr

October 16, 2023

Abstract

We introduce the *extremal range*, a local statistic for studying the spatial extent of extreme events in random fields on \mathbb{R}^2 . Conditioned on exceedance of a high threshold at a location s , the extremal range at s is the random variable defined as the smallest distance from s to a location where there is a non-exceedance. We leverage tools from excursion-set theory to study distributional properties of the extremal range, propose parametric models and predict the median extremal range at extreme threshold levels. The extremal range captures the rate at which the spatial extent of conditional extreme events scales for increasingly high thresholds, and we relate its distributional properties with the bivariate tail dependence coefficient and the extremal index of time series in classical Extreme-Value Theory. Consistent estimation of the distribution function of the extremal range for stationary random fields is proven. For non-stationary random fields, we implement generalized additive median regression to predict extremal-range maps at very high threshold levels. An application to two large daily temperature datasets, namely reanalyses and climate-model simulations for France, highlights decreasing extremal dependence for increasing threshold levels and reveals strong differences in joint tail decay rates between reanalyses and simulations.

Keywords: asymptotic dependence; climate extremes; excursion sets; intrinsic volumes; stochastic geometry; temperature data; threshold exceedances.

*The authors gratefully acknowledge that this work has been supported by the French government, through the 3IA Côte d'Azur Investments in the Future project managed by the National Research Agency (ANR) with the reference number ANR-19-P3IA-0002. French weather data based on the SAFRAN re-analysis model were made available by Météo France within its cooperation framework with INRAE. Contributions to the Mathematics Stack Exchange by Willie W.Y. Wong were highly influential in constructing the proof of Lemma 1.

1 Introduction

Assessing the spatial and temporal correlation of extreme events is an important modeling step in applications of environmental statistics where extreme risks arise from concurrence and compounding of extremes (Dombry et al. 2018, AghaKouchak et al. 2020). We here focus on assessing the spatial contiguity of extreme events based on excursion sets with the aim to avoid strong parametric assumptions and high numerical cost when inferring spatial extremal dependence properties from large datasets on regular grids. Analysis of excursion sets has become valuable in spatial statistics (e.g., Bolin & Lindgren 2015, Sommerfeld et al. 2018) and computer vision (e.g., Bleau & Leon 2000, Sezgin & Sankur 2004), especially for data on regular grids, such as climate model output, remote sensing data or medical images. We use the framework of Extreme-Value Theory (EVT, de Haan & Ferreira 2006), useful to formulate general tail-regularity assumptions and enable statistical extrapolation towards very high and even yet unobserved quantiles. The standard asymptotic models in spatial EVT exhibit asymptotic dependence where the limiting dependence structure of threshold exceedances is characterized by peaks-over-threshold stability (Ferreira & de Haan 2014, Dombry & Ribatet 2015, Thibaud & Opitz 2015). However, strong empirical evidence from many environmental processes advises against this property (Tawn et al. 2018, Huser & Wadsworth 2022). Often, spatial dependence between threshold exceedances is lost as thresholds are increased, and it may ultimately vanish in the case of asymptotic independence. More flexible subasymptotic models have been proposed to accommodate asymptotic independence or even both situations of asymptotic (in)dependence (Huser et al. 2017, Huser & Wadsworth 2022, Zhang et al. 2022).

Here, we use a setting borrowing from the idea of spatial conditional extremes (Heffernan & Tawn 2004, Wadsworth & Tawn 2022) to better understand spatial joint tail decay behavior near a location of interest. The tail dependence coefficient $\lim_{u \rightarrow 1} \mathbb{P}(F_2(X_2) > u \mid F_1(X_1) > u)$ of two random variables $X_i \sim F_i$, $i = 1, 2$, is a conditional probability that is a routinely used exploratory and diagnostic tool to assess the strength of bivariate extremal dependence (Coles et al. 1999). In spatial statistics, however, one usually has access to observations for a relatively large number of locations, and so methods of assessing extremal dependence based only on pairwise observations exclude pertinent information about multivariate, or spatial dependence structure, and numerical computation may become very costly for data available on regular grids with a large number of locations. There have been a number of methods to overcome this issue. Wadsworth & Tawn (2022), Simpson et al. (2023), for example, propose a parametric inference method based on a spatial extension of the multivariate conditional extremes model of Heffernan & Tawn (2004), which also relies on conditioning on an exceedance in one of the variables. Other works based on the conditional extremes model are limited in their applicability to high-dimensional datasets. As noted by Wadsworth & Tawn (2022), it is common in environmental data for the spatial dependence

to weaken as the considered threshold increases. One interpretation of this phenomenon, the inspiration for the statistics introduced in this paper, is that the *spatial extent* of extreme events tends to decrease with an increase in the threshold level. Thus, in this paper, we focus on the size and other geometric properties of excursion sets of continuous planar random fields—the regions where the random fields exhibit threshold exceedances. There is a vast literature concerning the geometric features of excursion sets of random fields; see [Adler & Taylor \(2007\)](#) for a comprehensive introduction. For smooth random fields, geometric summaries of excursion sets, namely their intrinsic volumes, carry pertinent information about the asymptotic dependence structure at extreme thresholds ([Di Bernardino et al. 2022](#)). In this paper, we introduce a new local statistic, the *extremal range*. The extremal range at a site $s \in \mathbb{R}^2$ is defined as the largest radius r around s such that all locations within r are extreme, conditioned on a threshold exceedance at s . We will explore how the extremal range relates to the intrinsic volumes of the excursion set and to the notion of asymptotic dependence defined by a positive value of the tail dependence coefficient.

The extremal range can be seen as a spatial analogue to the extremal index ([Moloney et al. 2019](#)), a popular asymptotic statistic for time series extremes that allows for interpretation as the reciprocal of the average number of consecutive time steps over which an extreme cluster spans. In this sense, both quantities provide a notion of the size of clusters of extremes. However, several notable distinctions can be made. Firstly, we consider two-dimensional Euclidean space and not one single time dimension with regular discrete time steps. In one dimension, the distributional properties of the extremal range and its asymptotics at high thresholds can be obtained by studying sojourn times of one dimensional stochastic processes ([Berman 1971, 1982](#), [Kratz 2006](#), [Pham 2013](#), [Dalmao et al. 2019](#)). Where the classical extremal index is equal to unity in the case of asymptotic independence and therefore not informative, the extremal range can be used to quantify the degree of asymptotic dependence for asymptotically independent random fields. An important practical difference further stems from the fact that edge effects at the boundary of the observation window play a more important role in the spatial setting than in the temporal one. Thus, for spatial environmental datasets, care needs to be taken when computing the extremal range when the surrounding data is censored or unavailable.

Our results are organized as follows. §2 introduces the extremal range and notations. In §3, we express the cumulative distribution function of the extremal range through the intrinsic volumes of the excursion regions. In §4, we study the asymptotic behavior of the extremal range for common random field models as the threshold at the conditioning location s is increased, and propose a parametric model for the quantiles of the extremal range. Inference methods for estimating the extremal range and its quantiles are described in §5, and are applied to French temperature data by using a generalized additive quantile

regression framework in §6. Some technical definitions and examples are postponed to Appendix A. Finally, proofs and supporting lemmas for the theory established in §§3, 4, and 5 are provided in Appendix B.

2 The extremal range and relevant notations

Let $(\Omega, \mathcal{F}, \mathbb{P})$ be a probability space and let $X : \Omega \times \mathbb{R}^2 \rightarrow \mathbb{R}$ be a random field defined on \mathbb{R}^2 , the Euclidean plane, endowed with the Euclidean metric $\|\cdot\|$ and Lebesgue measure $\mathcal{L}(\cdot)$. For a study domain $S \subseteq \mathbb{R}^2$, let ∂S denote its topological boundary. For $x \in \mathbb{R}^2$, denote the distance between x and a non-empty set S by $\text{dist}(x, S) := \inf\{\|x - s\| : s \in S\}$. Throughout this paper, $u : \mathbb{R}^2 \rightarrow \mathbb{R}$ denotes a deterministic threshold that is allowed to vary in space, and we focus on the binary random field of excursion indicators $\{X(t) > u(t)\}_{t \in \mathbb{R}^2}$. This is expressed in terms of the following definition.

Definition 1 (Excursion set). *Let X be a random field on \mathbb{R}^2 and $u : \mathbb{R}^2 \rightarrow \mathbb{R}$ be a threshold function that may vary in space. Define the excursion set of X to be*

$$E_X(u) := \{t \in \mathbb{R}^2 : X(t) > u(t)\}.$$

Definition 2 (Extremal range). *For $r > 0$ and $s \in \mathbb{R}^2$, let $B(s, r) := \{t \in \mathbb{R}^2 : \|t - s\| \leq r\}$ denote the closed ball of radius r centered at s . Let $\tilde{R}^{(u)} : \Omega \times \mathbb{R}^2 \rightarrow \mathbb{R}^+ \cup \{0, \infty\}$ be a random field defined by*

$$\tilde{R}^{(u)}(t) := \sup\{r \in \mathbb{R}^+ : B(t, r) \subset E_X(u)\} = \text{dist}(t, (E_X(u))^c), \quad t \in \mathbb{R}^2.$$

Let $s \in \mathbb{R}^2$ satisfy $u(s) < x^(s)$, with $x^*(s) := \inf\{x \in \mathbb{R} : \mathbb{P}(X(s) > x) = 0\}$ denoting the upper end-point of the marginal density of X at s . Define the extremal range at s , denoted $R_s^{(u)}$, to be the random variable whose pushforward measure is given by*

$$\mathbb{P}(R_s^{(u)} \in A) = \mathbb{P}(\tilde{R}^{(u)}(s) \in A \mid X(s) > u(s)), \quad A \in \mathcal{B}(\mathbb{R}).$$

Remark 1. As discussed in Moloney et al. (2019), the inverse of the so-called extremal index quantifies the average size of clusters of threshold exceedances for time series, *i.e.*, for one-dimensional discrete random processes. Analogously, the extremal range provides a notion of the size of the clusters of sites that exhibit threshold exceedances for continuous, two-dimensional random fields.

The definitions below are relevant to establish the main results for the extremal range.

Definition 3 (Erosion and dilation). *For two nonempty sets $A, B \subseteq \mathbb{R}^2$, let $A \oplus B := \{x + y : x \in A, y \in B\}$ be the Minkowski sum of A and B . For $r \in \mathbb{R}$, and $S \subseteq \mathbb{R}^2$ let*

$$S_r := \begin{cases} S \oplus B(0, r), & \text{for } r \geq 0, \\ (S^c \oplus B(0, -r))^c, & \text{for } r < 0, \end{cases}$$

denote respectively the set dilation and the set erosion, depending on the sign of r .

Definition 4 (Connected components of the level set). *Let $T \subset \mathbb{R}^2$ be compact and define $N_T^{(u)}$ to be the number of connected components of the level curve $\partial E_X(u) \cap T$.*

Definition 5 (Lipschitz-Killing curvature densities). *For a set $S \subset \mathbb{R}^2$, let $\chi(S)$ denote the Euler-Poincaré characteristic of S (equal to the number of connected components of S minus the number of holes in S) and let $\ell(\partial S)$ denote the perimeter length of S (the one-dimensional Hausdorff measure of its boundary). Recall that \mathcal{L} denotes the Lebesgue measure. For a compact set $T \subset \mathbb{R}^2$ with positive Lebesgue measure, assuming the limits exist, define the curvature densities,*

$$\begin{aligned} C_0^*(E_X(u)) &:= \lim_{n \rightarrow \infty} \frac{\mathbb{E}[\chi(E_X(u) \cap nT)]}{\mathcal{L}(nT)}, \\ C_1^*(E_X(u)) &:= \lim_{n \rightarrow \infty} \frac{\mathbb{E}[\ell(\partial(E_X(u) \cap nT))]}{2\mathcal{L}(nT)}, \\ C_2^*(E_X(u)) &:= \lim_{n \rightarrow \infty} \frac{\mathbb{E}[\mathcal{L}(E_X(u) \cap nT)]}{\mathcal{L}(nT)}, \end{aligned}$$

where nT is the result after linearly rescaling T by n .

Note that $C_i^*(E_X(u))$, for $i = 0, 1, 2$, are the limiting normalized intrinsic volumes of the excursion set $E_X(u)$ seen on large domains (Schneider & Weil 2008, Theorem 9.3.3). They play an important role in determining the shape of the distribution function of the extremal range; a topic that we investigate in the following section.

3 Linking the extremal range and intrinsic volumes

Proposition 1. *Suppose that the random field X is continuous and stationary, and that u is constant and less than $x^*(0)$. For any compact set $T \subset \mathbb{R}^2$ with $\mathcal{L}(T) > 0$, the distribution function of $R_0^{(u)}$ is given by*

$$\mathbb{P}(R_0^{(u)} \leq r) = 1 - \frac{\mathbb{E}[\mathcal{L}(E_X(u)_{-r} \cap T)]}{\mathbb{E}[\mathcal{L}(E_X(u) \cap T)]}, \quad (1)$$

for $r \geq 0$, and $\mathbb{P}(R_0^{(u)} < 0) = 0$, where the subscript $-r$ denotes set erosion by a radius of r (see Definition 3, Equation (1)).

The proof of Proposition 1 is provided in Appendix B.1. The extremal range has close links with the *spherical erosion function* (Serra 1984, Ripley 1988), which describes the distribution function of the distance of a uniform random point in a set to the set's boundary. Proposition 1 states that the eroded excursion set $E_X(u)_{-r}$ carries information about the distribution of $R_s^{(u)}$ through its area when intersected with a compact set T . Areas of excursion sets and their erosion can be efficiently estimated with routine algorithms,

such that Equation (1) can be used for estimating the distribution function of $R_0^{(u)}$ in the stationary setting by replacing expectations with empirical estimates.

Next, we show that under certain regularity conditions, a polynomial expression of the Lebesgue measure of an eroded set in terms of its Lipschitz-Killing curvatures (see Definition 5) can be obtained as corollary to the well-known Steiner formula (Federer 1959, Theorem 5.6). The most general case for which this is known to hold is when the complement of the considered set has *positive reach* (see Definition 9 in Appendix A.1).

Assumption 1. *Suppose that for the random field X paired with the threshold function u , the excursion set $E_X(u)$ is a stationary random set. In addition, for any compact, convex $T \subset \mathbb{R}^2$ with positive Lebesgue measure, suppose that*

- *the densities in Definition 5 exist, are finite, and are independent of T ;*
- *$E_X(u)^c \cap T$ is almost surely a positive reach set;*
- *$\mathbb{E}[N_T^{(u)}] < \infty$ (see Definition 4).*

Under Assumption 1, the random field X is not necessarily stationary, as u is not necessarily a constant function in space. What is necessary instead is that the *excursion set* at the level u be stationary. An important, easily verifiable consequence of this is that $C_2^*(E_X(u)) = \mathbb{P}(X(0) > u(0))$. The condition that $E_X(u)^c \cap T$ is positive reach implies a certain regularity or smoothness of $\partial E_X(u)$. Conversely, compact subsets of \mathbb{R}^2 with a C^2 smooth boundary have positive reach (Thäle 2008, Proposition 14). Assumption 1 also implies that $E_X(u)$ is almost surely open, as its complement must be closed to satisfy the positive reach property. Examples of random fields that satisfy the last item in Assumption 1 are the Gaussian fields discussed in Beliaev et al. (2020). However, Gaussianity is not a necessary condition for our results, except for Proposition 2 focusing on results for such fields. A final remark on Assumption 1 is that it allows for the random fields X and $X - u$ to be discontinuous with positive probability.

An important property of the extremal range under Assumption 1 is asserted by the following Lemma, which we prove in Appendix B.1.

Lemma 1. *Under Assumption 1, $\mathbb{P}(R_0^{(u)} \leq r)$ is continuous in r , for $r > 0$.*

The main result of this section is the following first-order approximation of the distribution function of the extremal range. The proof of Theorem 1 can be found in Appendix B.1.

Theorem 1. *Under Assumption 1, for $r > 0$, it holds that*

$$\frac{\mathbb{P}(R_0^{(u)} \leq r)}{r} \xrightarrow{r \rightarrow 0} \frac{2C_1^*(E_X(u))}{C_2^*(E_X(u))}. \quad (2)$$

Theorem 1 shows that the distribution of the extremal range follows a first-order Taylor expansion for positive values of the radius r near 0. Moreover, the linear coefficient is provided by the limit on the right-hand side of Equation (2). By studying how this coefficient behaves for large thresholds, we gain insight about the spatial extent of high threshold exceedances.

4 The asymptotic behavior of the extremal range

We study the asymptotic behavior of the extremal range as the threshold function u tends to the location-wise upper endpoint of the distribution of X everywhere in space. By studying the extremal range, we aim to capture information about the dependence structure of the random field X . Therefore, we use the threshold function $u_p : \mathbb{R}^2 \rightarrow \mathbb{R}$ defined below as a location-wise quantile, such that it naturally adapts to the margins of the random field X .

Definition 6. For $p \in (0, 1)$ and a random variable $Y : \Omega \rightarrow \mathbb{R}$, let $q_p(Y) \in \mathbb{R}$ denote the p -quantile of Y , i.e., $q_p(Y) := \inf\{r \in \mathbb{R} : \mathbb{P}(Y \leq r) \geq p\}$. Now, define the adaptive threshold u_p by the mapping $u_p(s) := q_p(X(s))$, for $s \in \mathbb{R}^2$.

Theorem 1 allows us to study how the extremal range decreases as the considered threshold increases, i.e., as $p \rightarrow 1$. This important result is summarized in the following corollary.

Corollary 1. Suppose that Assumption 1 holds for the threshold function u_p , for all sufficiently large $p \in (0, 1)$. Then a function $g : (0, 1) \rightarrow \mathbb{R}$ satisfies

$$\lim_{p \rightarrow 1} g(p) \frac{C_2^*(E_X(u_p))}{2C_1^*(E_X(u_p))} = \frac{1}{K}, \quad (3)$$

for some $K \in \mathbb{R}^+$, if and only if

$$\lim_{p \rightarrow 1} \lim_{r \rightarrow 0} \frac{\mathbb{P}(g(p)R_0^{(u_p)} \leq r)}{r} = K. \quad (4)$$

Proof. Theorem 1 tells us that for any p ,

$$\lim_{r \rightarrow 0} \frac{\mathbb{P}(g(p)R_0^{(u_p)} \leq r)}{r} = \frac{2C_1^*(E_X(u_p))}{g(p)C_2^*(E_X(u_p))}.$$

Sending $p \rightarrow 1$ yields the desired result. \square

An interpretation of Corollary 1 is that the probability density function of $g(p)R_0^{(u_p)}$ just to the right of 0 approaches 1 if and only if $g(p)$ is asymptotically equivalent to $2C_1^*(E_X(u_p))/C_2^*(E_X(u_p))$ as $p \rightarrow 1$. In this sense, Corollary 1 shows how $R_0^{(u_p)}$ scales as $p \rightarrow 1$. We are not able to use Corollary 1 to establish a non-degenerate limit distribution of $[2C_1^*(E_X(u_p))/C_2^*(E_X(u_p))]R_0^{(u_p)}$ as $p \rightarrow 1$; it is not always possible to exchange the order of the limits in Equation (4). A counterexample is provided in Appendix A.2.

4.1 Non-degenerate limit distributions of the extremal range

Here, we study certain cases of widely used spatial random field models where the extremal range is known to have a non-degenerate limit distribution at high thresholds after appropriate rescaling. This will serve as basis for defining parametric statistical models for the extrapolation behavior of the extremal range at extreme conditioning thresholds. The random fields that we will consider in this section are stationary, so we choose a threshold function u that is constant throughout space. To ease notation, we write u to denote both the constant mapping $u : \mathbb{R}^2 \rightarrow \mathbb{R}$ and its image in \mathbb{R} .

4.1.1 Gaussian random fields

For a smooth, stationary Gaussian process Y on \mathbb{R} , if one is to condition on the event $\{X(0) > u\}$ for some large threshold $u \in \mathbb{R}$, one can show using tools developed in [Kac & Slepian \(1959\)](#) that the connected component of the excursion set containing 0 is a random interval with expected length asymptotically equivalent to $1/u$. By analogy, after appropriately rescaling in the spatial dimension, one finds that the limit process is a random parabola with deterministic shape. These insights are formally generalized for the two-dimensional case in the following proposition formulated for smooth standard Gaussian fields, for which a proof is given in [Appendix B.2](#).

Proposition 2. *Suppose that X is a stationary, isotropic, centered Gaussian random field on \mathbb{R}^2 with covariance function*

$$\rho(h) = 1 - \frac{\alpha}{2} \|h\|^2 + o(\|h\|^2), \quad \alpha > 0, \quad (5)$$

for h in a neighbourhood of 0. Then $\mathbb{P}(uR_0^{(u)} \in \cdot)$ converges to a non-degenerate probability distribution, as $u \rightarrow \infty$.

A stationary, isotropic Gaussian random field with unit variance and C^1 -smooth sample paths has the covariance function in (5) with α equal to its second spectral moment; see [Leadbetter et al. \(1983, page 151\)](#) and [Cambanis \(1973\)](#). The isotropic, Matérn covariance function

$$\rho(h) = \frac{2^{1-\nu}}{\Gamma(\nu)} \left(\frac{\sqrt{2\nu} \|h\|}{l} \right)^\nu K_\nu \left(\frac{\sqrt{2\nu} \|h\|}{l} \right), \quad \nu, l > 0,$$

with K_ν denoting the modified Bessel function of the second kind, satisfies (5) for $\nu > 1$ and

$$\alpha = \frac{\nu}{l^2(\nu - 1)}.$$

For a random field X as described in [Proposition 2](#), the expressions for $C_1^*(E_X(u))$ and $C_2^*(E_X(u))$ are computed in [Biermé et al. \(2019\)](#) using the Gaussian Kinematic Formula

(Adler & Taylor 2007, Theorem 15.9.5). By the results of Gordon (1941) concerning the Mill's ratio of the Gaussian distribution,

$$\frac{2C_1^*(E_X(u))}{C_2^*(E_X(u))} = \frac{\sqrt{\alpha}e^{-u^2/2}}{2(1 - \Phi(u))} \sim \sqrt{\frac{\pi\alpha}{2}}u,$$

where Φ denotes the standard Gaussian cumulative distribution function, and α is as in (5). Therefore, by using Corollary 1 with $g(p) = u_p(0)$, the probability density of $uR_0^{(u)}$ just to the right of 0 approaches $\sqrt{\pi\alpha/2}$, as $u \rightarrow \infty$. If one were to show in addition the uniform convergence of the density of the extremal range, one may conclude that $\sqrt{\pi\alpha/2}$ is the limiting value as $r \rightarrow 0$ of the limiting density, as $u \rightarrow \infty$.

In practice, a useful approximation of the distribution function $R_0^{(u)}$ for large u and small r for Gaussian random fields is therefore

$$\mathbb{P}(R_0^{(u)} \leq r) \approx \sqrt{\frac{\pi\alpha}{2}}ur,$$

where an estimate $\hat{\alpha}$ of the second spectral moment α based on a parametric covariance function $\rho(h)$ could be plugged in to obtain an estimate for spatial data corresponding to relatively smooth spatial surfaces.

4.1.2 Regularly varying fields

Here, we recall the core elements of the theory of regularly varying random fields, and the related ℓ -Pareto processes from Ferreira & de Haan (2014), Dombry & Ribatet (2015), commonly used as models for spatial processes conditioned on high threshold exceedances of a certain cost functional.

Let T be a compact domain satisfying $r_T := \sup\{r \in \mathbb{R}^+ : B(0, r) \subseteq T\} > 0$. Let X be a continuous, stationary random field defined on \mathbb{R}^2 , and let $X|_T$ be the random field X restricted to the domain T . Let \mathcal{C}_0 be the set of continuous functions from T to $[0, \infty)$, excluding the constant function 0. Let $\mathcal{S} = \{x \in \mathcal{C}_0 : \|x\|_T = 1\}$, where $\|x\|_T := \sup_{t \in T} x(t)$.

In Appendix A.3, we recall from Dombry & Ribatet (2015) what it means for a random field to be *regularly varying with exponent α and spectral measure σ on \mathcal{S}* . The limiting behaviour of these random fields at high thresholds can be well described by *ℓ -Pareto random fields* (see Lemma 5 in Appendix B.3); more recently also called *r -Pareto random fields* with r standing for *risk* (de Fondeville & Davison 2022). These random fields are characterized by a *cost functional* $\ell : \mathcal{C}_0 \rightarrow [0, \infty)$ that is homogeneous of order 1, *i.e.*, $\ell(ux) = u\ell(x)$ for all $x \in \mathcal{C}_0$ and $u > 0$. The precise definition of an ℓ -Pareto random field is provided in Definition 10 in Appendix B.3. For now, we borrow the notation of Dombry & Ribatet (2015) and write $\mathbb{P}_{\alpha, \sigma_\ell}^\ell$ for the set of ℓ -Pareto random fields with exponent α and spectral measure σ_ℓ .

For regularly varying X , it is possible to express the limit distribution of the extremal range in terms of two different constructions of ℓ -Pareto processes.

Proposition 3. *Suppose that $X|_T$ is regularly varying with exponent $\alpha > 0$ and spectral measure σ on \mathcal{S} . Define the cost functionals f and g mapping from \mathcal{C}_0 to $[0, \infty)$ by $f : x \mapsto \|x\|_T$ and $g : x \mapsto x(0)$, and let $Y_T \in \mathbb{P}_{\alpha, \sigma_f}^f$, and $Y_0 \in \mathbb{P}_{\alpha, \sigma_g}^g$. Here, $\sigma_f(A) := \sigma(\mathcal{S} \cap A) / \sigma(\mathcal{S})$ and $\sigma_g(A) := \frac{1}{c} \int_{\mathcal{S}} x(0)^\alpha \mathbb{1}_{\{x/x(0) \in A\}} \sigma(dx)$ for $A \in \mathcal{B}(\mathcal{C}_0)$, with $c := \int_{\mathcal{S}} x(0)^\alpha \sigma(dx)$. Then, for $r \in (0, r_T)$,*

$$\lim_{u \rightarrow \infty} \mathbb{P}(R_0^{(u)} \leq r) = 1 - \frac{\mathbb{E}[\mathcal{L}((E_{Y_T}(1) \cap T)_{-r})]}{\mathcal{L}(T_{-r}) \mathbb{P}(Y_T(0) > 1)} = \mathbb{P}(\exists t \in B(0, r) \text{ s.t. } Y_0(t) \leq 1). \quad (6)$$

The proof of Proposition 3 is postponed to Appendix B.3.

4.2 Connections with the tail dependence coefficient

Taking a more non-parametric perspective, we continue using the threshold function u_p as defined in Definition 6 that adapts to non-stationary random fields.

Recall that for two sites $s_1, s_2 \in \mathbb{R}^2$, the tail dependence coefficient function of a spatial random field X is defined as $\chi(s_1, s_2) := \lim_{p \rightarrow 1} \chi_p(s_1, s_2)$, where,

$$\chi_p(s_1, s_2) := \frac{\mathbb{P}(X(s_1) > u_p(s_1), X(s_2) > u_p(s_2))}{1 - p} = \mathbb{P}(X(s_1) > u_p(s_1) \mid X(s_2) > u_p(s_2)).$$

Here, we use the following definition of asymptotic (in)dependence. The random field X is said to be *asymptotically independent* if $\chi(s_1, s_2) = 0$ for all $s_1 \neq s_2$, and *asymptotically dependent* if $\chi(s_1, s_2) > 0$, for all $s_1, s_2 \in \mathbb{R}^2$. The asymptotic dependence of X forces the asymptotic behavior of $R_s^{(u)}$ as $u \rightarrow \infty$. Indeed, if X exhibits asymptotic independence, then we have immediately that $R_s^{(u)} \xrightarrow{\mathbb{P}} 0$, as $u \rightarrow \infty$. This simple observation is a corollary of the following proposition.

Proposition 4. *Let X be any random field on \mathbb{R}^2 . For all $s \in \mathbb{R}^2$ and all $p \in (0, 1)$,*

$$\mathbb{P}(R_0^{(u_p)} \leq \|s\|) \geq 1 - \chi_p(s, 0).$$

Proof. The event $\{\tilde{R}^{(u_p)}(0) > \|s\|, X(0) > u_p\}$ is contained in the event $\{X(s) > u_p, X(0) > u_p\}$. Therefore, $\mathbb{P}(\tilde{R}^{(u_p)}(0) > \|s\|, X(0) > u_p) \leq \mathbb{P}(X(s) > u_p, X(0) > u_p)$. A division by $\mathbb{P}(X(0) > u_p)$ (equal to $1 - p$ if $X(0)$ has a continuous distribution function) implies $\mathbb{P}(\tilde{R}^{(u_p)}(0) > \|s\| \mid X(0) > u_p) \leq \mathbb{P}(X(s) > u_p \mid X(0) > u_p)$, and the result holds by taking compliments. \square

Therefore, asymptotic dependence is a necessary condition for $R_0^{(u_p)}$ to have a non-degenerate limit distribution as $p \rightarrow 1$. However, it is not sufficient. In Appendix A.2, we study a random field for which $R_0^{(u_p)} \xrightarrow[p \rightarrow 1]{\mathbb{P}} 0$; the following theorem makes an important link between the extremal range and the tail dependence coefficient, and establishes that in this specific case, $\chi(0, s) = 1$ for all $s \in \mathbb{R}^2$.

Theorem 2. Let X be an isotropic random field, and suppose that for $p \in (0, 1)$, Assumption 1 is satisfied for the threshold function u_p . Let h be a real function of $p \in (0, 1)$ such that

$$h(p) \frac{C_2^*(E_X(u_p))}{C_1^*(E_X(u_p))} \xrightarrow{p \rightarrow 1} \infty.$$

Then, for any fixed $s \in \mathbb{R}^2$, $\chi_p(s/h(p), 0) \xrightarrow{p \rightarrow 1} 1$.

Proof. Assumption 1 provides an alternative set of hypotheses to support the result of [Cotsakis et al. \(2022, Theorem 2.1\)](#) which states that for $p \in (0, 1)$ and $s \in \mathbb{R}^2$,

$$\frac{1}{q} \mathbb{P}(X(qs) \leq u_p(qs), X(0) > u_p(0)) \xrightarrow{q \rightarrow 0} \frac{C_1^*(E_X(u_p))}{\pi} \|s\|,$$

and the limit is approached from below. Thus, for any $q \in \mathbb{R}^+$, a division by $1 - p$ yields

$$\frac{1 - \chi_p(qs, 0)}{q} \leq \frac{C_1^*(E_X(u_p))}{C_2^*(E_X(u_p))\pi} \|s\|.$$

By setting $q = 1/h(p)$, we find that

$$1 - \chi_p(s/h(p), 0) \leq \frac{C_1^*(E_X(u_p))}{h(p)C_2^*(E_X(u_p))\pi} \|s\| \xrightarrow{p \rightarrow 1} 0.$$

The desired result holds since $\chi_p \in [0, 1]$ for all $p \in (0, 1)$. □

Remark 2. Recall that $2C_1^*(E_X(u_p))/C_2^*(E_X(u_p))$ is the limit value in Theorem 1, giving the first-order approximation of the cumulative distribution function of the extremal range. For many random fields, this is seemingly the rate at which space should be rescaled as $p \rightarrow 1$ if one is to expect the tail dependence coefficient and the distribution function of the extremal range to stabilize to values strictly between 0 and 1.

4.3 A parametric model for the extremal range

We have seen that tail dependence coefficient determines whether a random field is asymptotically dependent or independent according to our definition. While it is natural to study pairwise exceedances in discrete data, an attractive alternative is to describe the spatial dependence of continuous data using the extremal range. The extremal range tends to 0 in probability as higher thresholds are considered for asymptotically independent random fields; see Proposition 4. The rate of this convergence provides an alternative, more precise notion of extremal independence. To formalize this idea, we propose the following assumption on the random field X .

Assumption 2. For each $s \in \mathbb{R}^2$, the distribution of $R_s^{(u_p)}$ is non-degenerate for $p \in (0, 1)$, and there exists $\theta_s \in [0, \infty)$ such that for all $a > 0$ and $\alpha \in (0, 1)$,

$$\frac{q_\alpha(R_s^{(u_{p'})})}{q_\alpha(R_s^{(u_p)})} \xrightarrow{p \rightarrow 1} a^{-\theta_s},$$

where $p' = 1 - (1 - p)^a$.

Assumption 2 is equivalent to demanding that the quantile functions $q_\alpha(R_0^{(u)})$, for $\alpha \in (0, 1)$, $u \in \mathbb{R}^+$, are regularly varying in u after X is transformed to have standard exponential margins. The indices of regular variation are allowed to vary throughout space. For asymptotically independent models, the quantile function $q_\alpha(R_s^{(u_p)})$ tends to decrease as $p \rightarrow 1$, and so one expects θ_s to be large. However, for asymptotically dependent models, the same quantile function approaches a positive constant as $p \rightarrow 1$, in which case, one can expect $\theta_s = 0$. Contrary to other popular measures of asymptotic dependence, θ_s distinguishes between varying degrees of asymptotic *independence*. A consistent, local estimator for θ_s is defined in §5.2, thus providing a measure of the spatial asymptotic independence at high thresholds.

In addition, §5.3 outlines how linear quantile regression can be used to extrapolate or interpolate the quantiles of the extremal range when the excursion sets are observed at multiple levels.

Remark 3. The Gaussian (resp. regularly varying) random fields studied in §4.1 satisfy Assumption 2 with $\theta_s = 1/2$ (resp. $\theta_s = 0$) for all $s \in \mathbb{R}^2$. Therefore, Assumption 2 can be applied to both asymptotically dependent and asymptotically independent models.

5 Inference

5.1 Empirical CDF of the extremal range for stationary fields

The results developed in §§3 and 4 lead to natural statistical procedures for estimating the extremal range. We begin by describing a simple procedure for strongly mixing sequences of random fields that are assumed to be stationary and identically distributed. Independent replications of the random field are trivially strongly mixing.

Proposition 5. *Let $T \subset \mathbb{R}^2$ be compact, and suppose that $\bar{r}_T := \sup\{r \in \mathbb{R}^+ : \mathcal{L}(T_{-r}) > 0\} > 0$. Let X_1, \dots, X_n be a strongly mixing sequence of random fields defined on T , each equal in distribution to the stationary random field X (Rosenblatt 1956). Define*

$$\tilde{R}_i^{(u)}(t) := \text{dist}(t, (E_{X_i}(u))^c), \quad (7)$$

for some threshold $u \in \mathbb{R}$ satisfying $\mathbb{P}(X(0) > u) > 0$, and

$$\hat{F}_n(r) := \begin{cases} \frac{\sum_{i=1}^n \mathcal{L}(\{t \in T_{-r} : 0 < \tilde{R}_i^{(u)}(t) \leq r\})}{\sum_{i=1}^n \mathcal{L}(E_{X_i}(u) \cap T_{-r})} & , \text{ if } \sum_{i=1}^n \mathcal{L}(E_{X_i}(u) \cap T_{-r}) > 0 \\ 0 & , \text{ if } \sum_{i=1}^n \mathcal{L}(E_{X_i}(u) \cap T_{-r}) = 0, \end{cases}$$

for $r \in (0, \bar{r}_T)$. It follows that $\hat{F}_n(r) \xrightarrow[n \rightarrow \infty]{\mathbb{P}} \mathbb{P}(R_0^{(u)} \leq r)$, uniformly for $r \in (0, \bar{r}_T)$.

Proof. Fix $r \in (0, \bar{r}_T)$ and $u \in \mathbb{R}$. By the strongly mixing assumption, the sequences $(\mathcal{L}(\{t \in T_{-r} : 0 < \tilde{R}_i^{(u)}(t) \leq r\}))_{i \geq 1}$ and $(\mathcal{L}(E_{X_i}(u) \cap T_{-r}))_{i \geq 1}$ are mean-ergodic, and so we write

$$\begin{aligned} \widehat{F}_n(r) &= \frac{\frac{1}{n} \sum_{i=1}^n \mathcal{L}(\{t \in T_{-r} : 0 < \tilde{R}_i^{(u)}(t) \leq r\})}{\frac{1}{n} \sum_{i=1}^n \mathcal{L}(E_{X_i}(u) \cap T_{-r})} \xrightarrow[n \rightarrow \infty]{\mathbb{P}} \frac{\mathbb{E}[\mathcal{L}(\{t \in T_{-r} : 0 < \tilde{R}^{(u)}(t) \leq r\})]}{\mathbb{E}[\mathcal{L}(E_X(u) \cap T_{-r})]} \\ &= \frac{\int_{T_{-r}} \mathbb{P}(0 < \tilde{R}^{(u)}(t) \leq r) dt}{\int_{T_{-r}} \mathbb{P}(X(t) > u) dt} = \frac{\mathbb{P}(\tilde{R}^{(u)}(0) \leq r, X(0) > u)}{\mathbb{P}(X(0) > u)} = \mathbb{P}(R_0^{(u)} \leq r). \end{aligned}$$

Uniform convergence follows from the continuity of the limiting distribution function (see Lemma 1) and Dini's theorem (Friedman 2007, p.199). \square

Proposition 5 therefore provides a convenient way to estimate the empirical distribution function of the extremal range under the assumption of stationarity for a series of time-replicated spatial fields.

5.2 Consistent estimation of the tail decay rate of the extremal range

Recall that under Assumption 2, the quantiles of the extremal range are parameterized by an index of regular variation θ_s for each site s in the study domain, which we call tail decay rate. We propose a local estimator for this quantity and show that it is consistent, providing the corresponding rate of convergence.

Definition 7. Let X_1, \dots, X_n be n realizations of the random field X . For $p \in (0, 1)$, define the empirical median of $R_s^{(u_p)}$ to be

$$\widehat{q}_{50\%}^{(n)}(R_s^{(u_p)}) := \operatorname{argmin}_{x \in \mathbb{R}^+} \left\{ \sum_{i=1}^n |x - \tilde{R}_i^{(u_p)}(s)| \mathbb{1}_{\{\tilde{R}_i^{(u_p)}(s) > 0\}} \right\},$$

with $\tilde{R}_i^{(u_p)}(s)$ as in (7). For $p_1, p_2 \in (0, 1)$, $p_1 \neq p_2$, define

$$\widehat{\theta}_s^{(n)}(p_1, p_2) = \frac{\log(\widehat{q}_{50\%}^{(n)}(R_s^{(u_{p_2})})) - \log(\widehat{q}_{50\%}^{(n)}(R_s^{(u_{p_1})}))}{\log(-\log(1 - p_1)) - \log(-\log(1 - p_2))}. \quad (8)$$

If $\tilde{R}_i^{(u_p)}(s) = 0$, $\forall i = 1, \dots, n$, for either $p = p_1$ or $p = p_2$, then both $\widehat{\theta}_s^{(n)}(p_1, p_2)$ and the empirical median $\widehat{q}_{50\%}^{(n)}(R_s^{(u_p)})$ are understood to be 0.

Proposition 6. Let X_1, \dots, X_n be n independent realizations of the random field X , satisfying Assumption 2. Fix $p_0 \in (0, 1)$, and let $(p_n)_{n \geq 1}$ be a sequence in $(0, 1)$ tending to 1 such that $n(1 - p_n) \rightarrow \infty$ as $n \rightarrow \infty$. Then, for each $s \in \mathbb{R}^2$, the estimator defined in (8) satisfies

$$\widehat{\theta}_s^{(n)}(p_0, p_n) \xrightarrow[n \rightarrow \infty]{\mathbb{P}} \theta_s,$$

where $\widehat{\theta}_s^{(n)}(p_0, p_n)$ is defined in Definition 7, and θ_s is defined in Assumption 2.

The proof of Proposition 6 can be found in Appendix B.4. The estimator in (8) can be viewed as the slope of a median regression with response $\log(\widehat{q}_{50\%}^{(n)}(R_s^{(u_{p_2})}))$ and covariate $\log(-\log(1-p_1))$. This motivates the following median regression approach for predicting the median extremal range at very extreme probability levels p close to 1.

5.3 Extrapolation for non-stationary data using median regression

As we have seen previously, under Assumption 1, the random excursion set $E_X(u)$ is stationary. This implies that the distribution of $R_s^{(u)}$ is invariant in the spatial location s , allowing one to extract information from the entire spatial domain to gain insights on the behavior of the extremal range at s . When $E_X(u)$ is non-stationary, it is likely that there is insufficient information to infer the entire distribution of $R_s^{(u)}$ (especially when $\mathbb{P}(X(s) > u(s))$ is small). Thus, it is reasonable to instead estimate a summary statistic of $R_s^{(u)}$. The median, $q_{50\%}(R_s^{(u)})$, is an appropriate statistic to estimate for several reasons: it is robust to censorship of large observations and to strongly discretized small values arising with data available on pixel grids; the median commutes with monotonic rescalings; one does not require the existence of moments of the distribution of the extremal range; the behavior of the median is controlled under Assumption 2 with $\alpha = 1/2$.

Definition 8. *The Median Extremal Range (MER) at a site $s \in \mathbb{R}^2$ at the threshold $u_p(s)$, for $p \in (0, 1)$, is defined as*

$$\text{MER}(s; p) := q_{50\%}(R_s^{(u_p)}).$$

Suppose that for several realizations X_1, \dots, X_n of X , the excursion set is observed at several high thresholds $u^{(1)}, \dots, u^{(k)}$. That is, we observe the sets $E_{X_i}(u^{(j)})$ for $(i, j) \in \{1, \dots, n\} \times \{1, \dots, k\}$. Under Assumption 2,

$$\frac{\log(\text{MER}(s; p')) - \log(\text{MER}(s; p))}{\log(-\log(1-p')) - \log(-\log(1-p))} \xrightarrow{p \rightarrow 1} -\theta_s, \quad (9)$$

for any $a \in (0, 1)$ (see Assumption 2). Thus, plotted on a log-log plot, the slope of the graph of the $\text{MER}(s; p)$ against $-\log(1-p)$ tends to a constant $-\theta_s$, as $p \rightarrow 1$. This justifies the use of quantile regression to estimate the median of our empirical observations of $\log \widetilde{R}^{(u_p)}(s)$ against $\log(-\log(1-p))$ for several $p \in (0, 1)$ moderately close to 1. In this way, the height of the resulting regression line provides a model for the median of $\log R^{(u_p)}(s)$. Exponentiating the regression line provides a model for the $\text{MER}(s; p)$ for arbitrarily large $p \in (0, 1)$ and therefore allows us to extrapolate extremal-range properties at very high quantile levels for which only few or no exceedances at all are available in

the data. Another important benefit of median regression that we can include covariates, such as the spatial coordinates, into the intercept and slope, and we can estimate nonlinear covariate effects thanks to generalized additive quantile regression, as highlighted in the following data application.

6 Application to gridded temperature data

We use the estimation methods introduced in §5 to identify the local spatial extent of extremes of daily average temperatures in climate model outputs and provide insights into their spatial patterns. Temperature is a weather variable that is known to vary relatively smoothly in space (Perkins et al. 2012). We study two datasets available for mainland France for a regular pixel grid at 8km resolution in the metric Lambert-II projection. The primary dataset is based on the SAFRAN reanalysis (Vidal et al. 2010) and spans the 1991–2020 period excluding 1997 and 1998. Reanalysis is climate model simulation conditioned on observational data, and is routinely used in climate-change impact studies as a proxy for real weather and climate. We compare our results for the reanalysis model to those obtained for temperatures simulated for the historical period 1951–2005 using a couple of Global-Circulation-Model and Regional-Climate-Model (*IPSL-WRF*), one of the reference models provided by the French weather service for studying climate change impacts (<http://www.drias-climat.fr/>), with data available on the same spatial grid as the SAFRAN reanalysis. We perform the same analyses for each of the two datasets, so that any differences in the results are due to statistical uncertainties (that we assess), and to fundamental differences in the distributional properties of the datasets.

We consider only data for summer months (June 1 to August 31) and assume temporal stationarity. We first estimate $u_p(s)$, the p -quantile of $X(s)$, for $p \in \{0.85, 0.86, \dots, 0.98\}$, using standard methods, for each location s separately. As we have preselected the summer months, during which the majority of temperature extremes typically manifest, it is justifiable to use a set of quantile levels including values that are relatively low for extreme-value analysis. This provides an estimate of the excursion set $E_X(u_p)$ for each day; see Figure 2. For each p and each pixel inside an excursion set, we estimate $\tilde{R}^{(u_p)}$ using the fast marching method (Sethian 1996) implemented in the R package `fastmaRching` (Silva & Steele 2014). To manage the absence of temperature data outside of France, we define our estimate of $\tilde{R}^{(u_p)}(s)$ to be the smallest distance from s to a site s' in mainland France with $X(s') \leq u_p(s')$. In terms of boundary effects, this is equivalent to considering the modified excursion set $E_X(u_p) \cup T^c$ with T corresponding to mainland France. The histograms of the empirical distribution of extremal ranges $\tilde{R}^{(u_p)}(s)$ —provided that $\tilde{R}^{(u_p)}(s) > 0$ —is shown in Figure 1 for the quantile levels $p = 0.85$ and $p = 0.98$, for all locations pooled together. We see a clear shift towards generally smaller extremal ranges at the higher threshold,

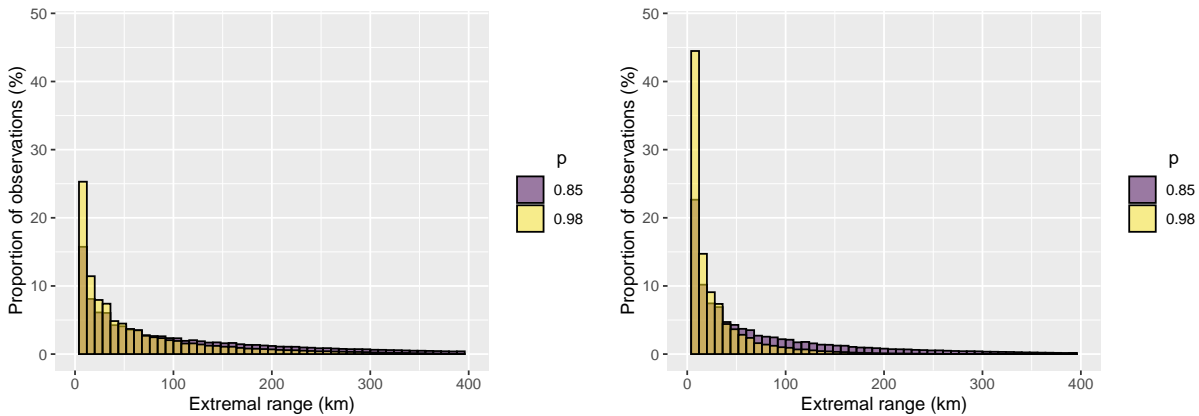


Figure 1: Histograms of estimated extremal ranges at two quantile levels for SAFRAN reanalysis (left) and IPSL-WRF simulations (right).

which means that dependence strength seems to decrease with the quantile level. Moreover, reanalysis data tend to have clearly larger extremal ranges than simulation data at both quantile levels, which hints at structural differences in the geometries of extremes among these two types of data, with generally smaller spatial clusters of extremes in the simulation data.

Next, we more precisely estimate the tail decay behavior of the extremal range and its spatial variability. Operating under Assumption 2, we estimate the parameters of a model for the $\text{MER}(s; p)$; see Definition 8. The model, as suggested by (9), is given by

$$\log(\text{MER}(s; p)) = \beta_s - \theta_s \log(-\log(1 - p)), \quad (10)$$

where the model parameters β_s and θ_s are allowed to vary over space. Using the set of estimates of $\tilde{R}^{(u_p)}$ for all p and all pixel-days in an excursion set, we use $\log \tilde{R}^{(u_p)}(s)$ —provided that $\tilde{R}^{(u_p)}(s) > 0$ —as the response variable in a generalized additive median regression with covariates s and $x := \log(-\log(1 - p))$. We implement a generalized additive model with spline tensor products defined over spatial coordinates for the parameters β_s and θ_s , such that their estimates vary smoothly in space (Wood 2017), *i.e.*, we perform a quantile regression with space-varying intercept and slope parameters. This modeling strategy would further allow for incorporating other covariates, such as altitude, or time to account for temporal trends.

We provide several diagnostic plots to illustrate the quantile regression fit. Figure 3 shows a satisfactory fit of the regression line for the SAFRAN data at two pixels s_1, s_2 with quite different intercept $\hat{\beta}_s$ and slope $\hat{\theta}_s$. Figure 4 provides maps of the estimates of the $\text{MER}(s; p)$ based on model (10) for two values of p . Standard deviations of estimates are computed using a block jackknife based on blocks given by years, where the whole chain of estimation is repeated for each jackknife sample. The resulting estimates of the $\text{MER}(s; p)$ correspond well with certain topographical features, even though this information was not

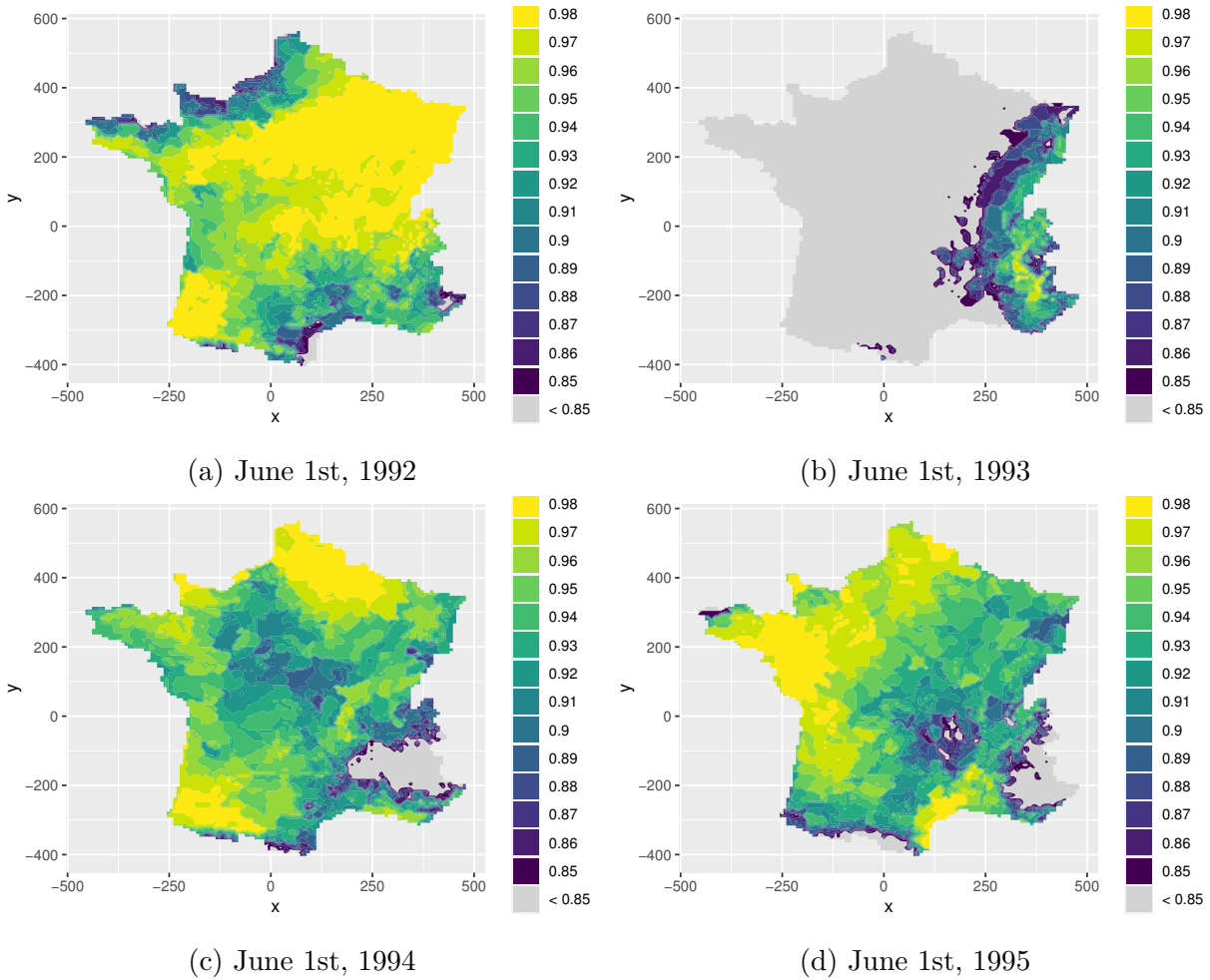


Figure 2: Realizations of nested excursion sets $E_X(u_p)$ for $p \in \{0.85, 0.86, \dots, 0.98\}$, for each of the four indicated dates in the SAFRAN reanalysis.

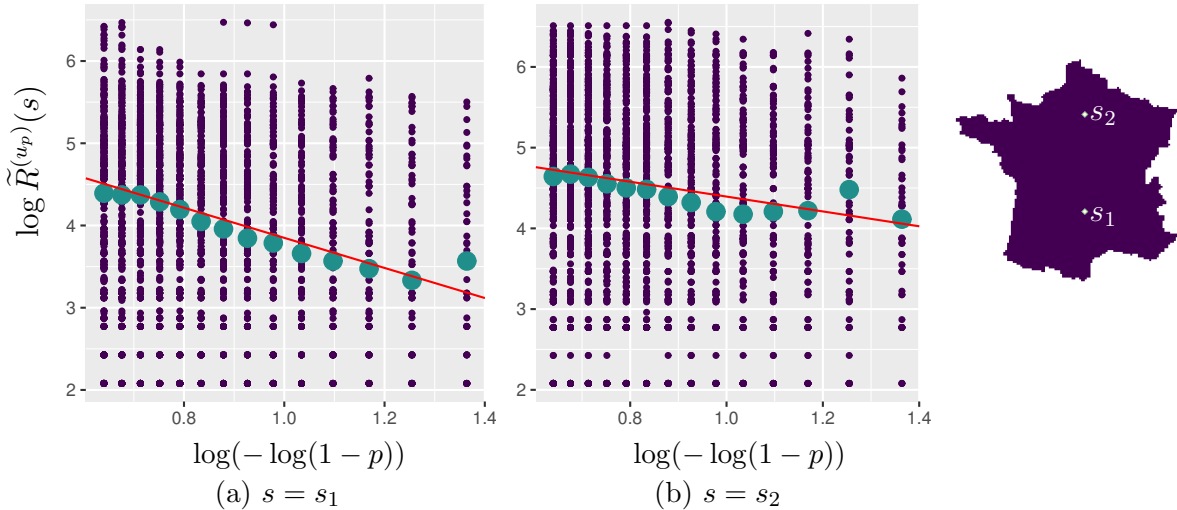


Figure 3: Illustration of median regression of the extremal range for SAFRAN reanalysis data. Fitted regression lines (red) of the model (10) for the log-median of the extremal range at the two sites s shown in the map on the right. For $p \in \{0.85, 0.86, \dots, 0.98\}$, we record a small blue point for all days where $\tilde{R}^{(u_p)}(s) > 0$, *i.e.*, where $X(s) > u_p(s)$. For each p , the empirical median of $\log \tilde{R}^{(u_p)}(s)$ is plotted as a larger green point to aid with visual diagnostic of the model fit. Multiplicity of points at discrete values is not shown.

provided to the model. The extremal range tends to be larger in planar regions, while it tends to be smaller in mountainous regions, and near the Atlantic coast to the East. Moreover, all jackknife-based estimates of the negative slopes θ_s , *i.e.*, of the tail decay rate, were positive, such that the signal against asymptotic dependence is significant around all pixels s . Figure 5 depicts the estimates of θ_s for the model (10), and their standard deviations. This parameter quantifies the joint tail decay rate near each location; see §4.3. As discussed previously, $\theta_s \leq 0$ implies asymptotic dependence, whereas $\theta_s > 0$ is a strong indicator of asymptotic independence, as the implication is in the reverse direction (see Proposition 4).

The results obtained for IPSL-WRF simulated temperatures differ quite drastically from those obtained for the SAFRAN reanalysis data. Estimated extremal ranges are substantially smaller for simulated temperatures and show less spatial variability and also differences in spatial patterns. Unless these differences arise from non-stationarity in time, our study demonstrates that the IPSL-WRF climate model has strong biases in the extremal range of temperatures when compared to the observation-based SAFRAN reanalysis.

7 Conclusion

The extremal range, particularly the evolution of the $\text{MER}(s;p)$ as $p \in (0,1)$ tends to 1, quantifies the degree of asymptotic independence locally at the site s . It aids flexible

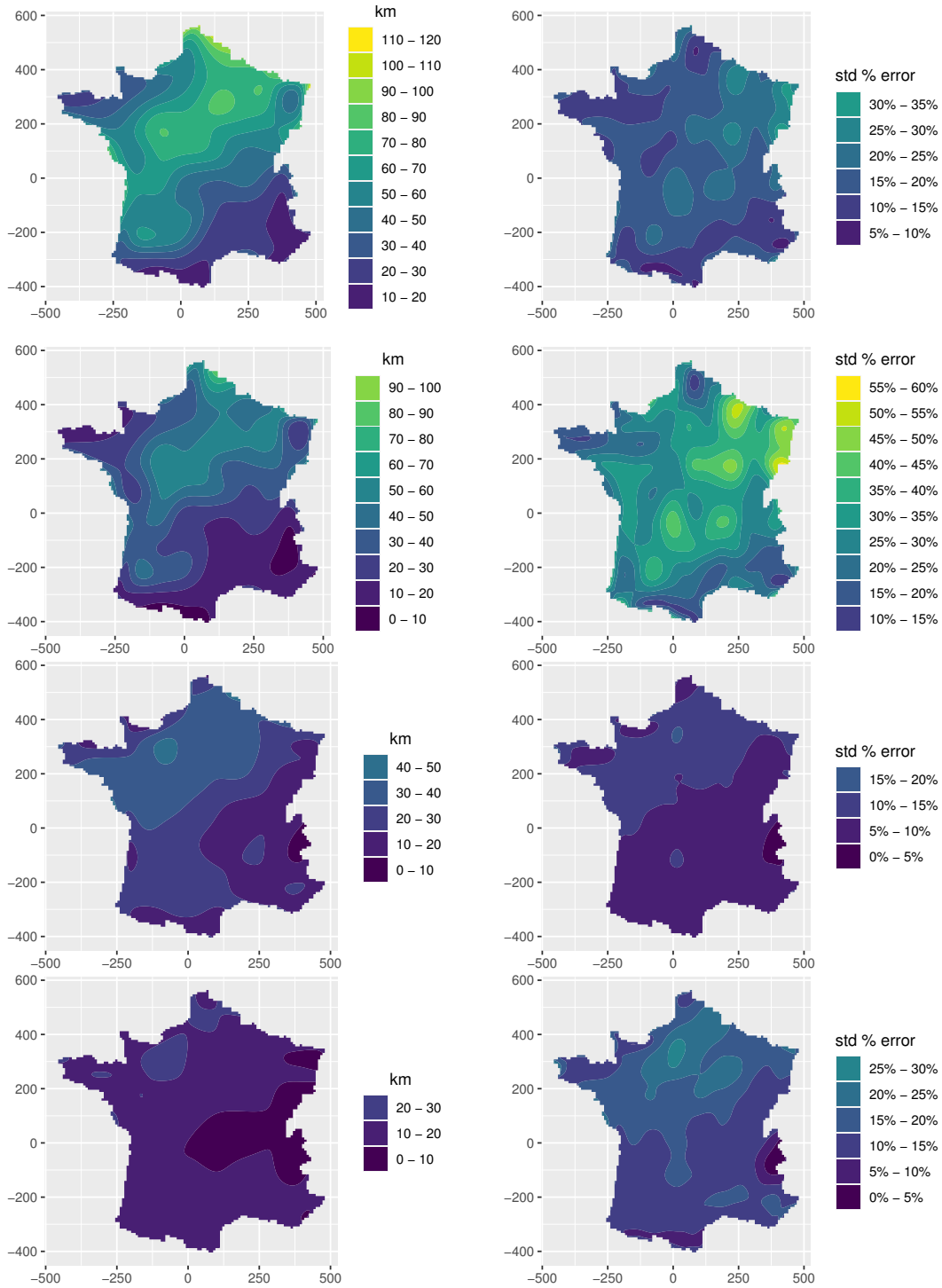


Figure 4: Estimates of the $MER(s; p)$ with relative standard errors (in %) for the SAFRAN reanalysis dataset for $p = 0.95$ (first row) and $p = 1 - 1/92 \approx 0.989$ (second row, corresponding to a one-year return level). The same quantities are computed for the IPSL-WRF simulated temperatures for $p = 0.95$ (third row) and $p = 1 - 1/92 \approx 0.989$ (fourth row). Color scales are the same across datasets and quantile levels.

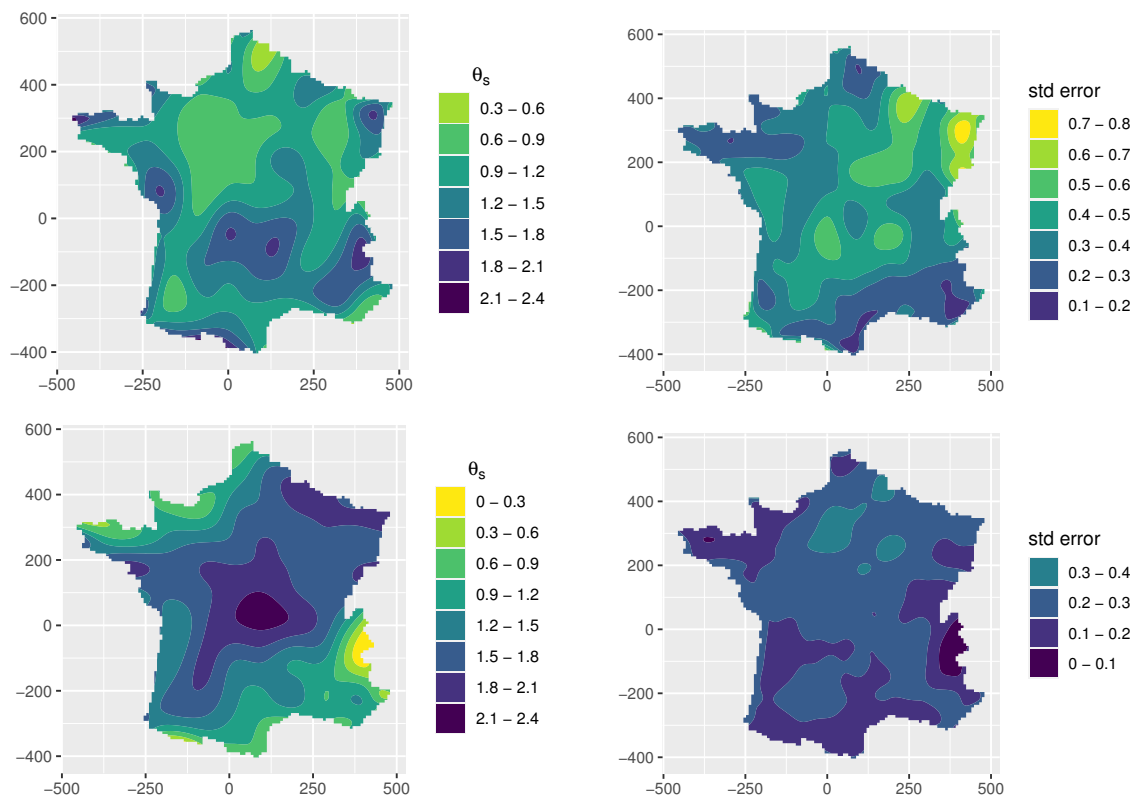


Figure 5: Estimates of the tail decay rate θ_s and its standard error for the SAFRAN reanalysis data (first row) and the IPSL-WRF simulated data (second row). The estimate is the negative slope of the model line in Figure 3. The larger θ_s , the less asymptotic dependence there is at the site s ; see §4.3. Color scales are the same for the two datasets.

exploratory analysis of dependence in spatial extremes beyond the mathematically elegant but rigid framework of asymptotically stable dependence in max-stable processes and other regularly varying processes. We have opted for the median as a summary parameter that allows for simple interpretation as a level that is on average exceeded in half of all cases of marginal exceedance at the reference location. It further allows for relatively robust estimation since it is less influenced by pixellization biases arising for small extremal ranges at lower quantiles and by boundary effects arising for large extremal ranges at higher quantiles. The proposed quantile regression approach further offers the possibility to include other covariates to model and explain non-stationary extremal dependence, such as temporal trends due to climate change. Our estimation methods scale well even for large gridded datasets with hundreds of thousands of pixels. By contrast with the common bivariate statistics defined as a function of spatial distance, our approach avoids the rather arbitrary and heuristic selection of location pairs to be considered for inferential purposes.

Data on regular grids at relatively high resolution, such as climate model output, provide a good approximation of the framework of continuous geographic space underpinning the concept of the extremal range. If data are not in this form, interpolation techniques such as kriging, piecewise linear interpolation based on Delaunay triangulation, or more sophisticated basis-function methods, could be applied first before conducting estimation of the extremal range.

While our focus was on descriptive statistics here, the extremal range could also be useful for generative modeling based on spatial random fields, for example by using $\text{MER}(s; p)$ as a goodness-of-fit diagnostics or as a covariate in the dependence structure.

The extremal range is a tool at the intersection of spatial EVT, stochastic geometry and topological data analysis. Further research in this area could help foster a high-dimensional statistical learning toolbox for studying complex structures in large volumes of climate data.

Appendix

A Technical definitions and examples

A.1 Positive reach

Definition 9. (*Federer 1959*) *The reach of a set $S \subseteq \mathbb{R}^2$ is given by $\sup\{r \in \mathbb{R} : \forall x \in S_r, \exists! s \in S \text{ nearest to } x\}$. A subset of \mathbb{R}^2 is termed positive reach if its reach is positive.*

Recall from [Federer \(1959\)](#) that a closed set is convex if and only if its reach is infinite. Therefore, the empty set is trivially a positive reach set.

A.2 A case where asymptotic dependence is not captured by the extremal range

Let $E \sim \text{Exp}(1)$, $\theta \in \text{Unif}([0, 2\pi])$, and $U \sim \text{Unif}([0, 1]^2)$ be independent, and consider the stationary, isotropic random field $\{X(t)\}_{t \in \mathbb{R}^2}$ defined by

$$X(t) = E \left(1 - \sum_{s \in \mathbb{Z}^2} \mathbf{1}_{\{\|s+U-ER_\theta(t)\| < 3^{-E}\}} \right),$$

where $R_\theta(t)$ is the image of t rotated by an angle θ about the origin. Notice that X satisfies Assumption 1, for if the excursion set is not empty, it is the complement of the union of disks of radius 3^{-E} with centers on a randomly oriented square grid with spacing E^{-1} . If for some $p \in (0, 1)$ we have $X(0) > u_p$, then $E > u_p$ and $X(R_{-\theta}(U)/E) = 0 \leq u_p$. Thus, $\tilde{R}^{(u_p)}(0) < \|U\|/E < \sqrt{2}/u_p$ which tends to 0 as $p \rightarrow 1$. Thus, $R_0^{(u_p)} \xrightarrow[p \rightarrow 1]{\mathbb{P}} 0$. It is not hard to check that

$$\frac{C_2^*(E_X(u_p))}{C_1^*(E_X(u_p))} \xrightarrow[p \rightarrow 1]{} \infty,$$

contrary to the behaviour of $R_0^{(u_p)}$.

A.3 Regularly varying random fields

The process $X|_T$ is said to be *regularly varying* with exponent α and spectral measure σ on \mathcal{S} if there exists a function $a : \mathbb{R}^+ \rightarrow \mathbb{R}^+$ such that $a(u) \rightarrow \infty$ and

$$u\mathbb{P}\left(\frac{1}{\|X\|_T}X|_T \in A, \|X\|_T > ra(u)\right) \rightarrow r^{-\alpha}\sigma(A)$$

as $u \rightarrow \infty$, for all $r > 0$ and $A \in \mathcal{B}(\mathcal{S})$ satisfying $\sigma(\partial A) = 0$ (see Definition 1 in [Dombry & Ribatet \(2015\)](#)). If $X|_T$ is regularly varying with exponent α and spectral measure σ , we write $X|_T \in \text{RV}_{\alpha, \sigma}(\mathcal{C}_0)$.

B Proofs and auxiliary results

B.1 Proofs for §3

Proof of Proposition 1. Since $R_0^{(u)}$ is almost surely non-negative, it suffices to check that (1) holds for $r \geq 0$. Note that by the continuity of X , the excursion set $E_X(u)$ is open,

and so the events $\{\tilde{R}_0^{(u)} > r\}$ and $\{B(0, r) \subset E_X(u)\}$ are equal. Furthermore,

$$\begin{aligned} \mathbb{P}(R_0^{(u)} > r) &= \mathbb{P}(B(0, r) \subset E_X(u) \mid X(0) > u(0)) = \frac{\mathcal{L}(T)\mathbb{P}(B(0, r) \subset E_X(u))}{\mathcal{L}(T)\mathbb{P}(X(0) > u(0))} \\ &= \frac{\mathbb{E}\left[\int_T \mathbf{1}_{\{B(t, r) \subset E_X(u)\}} dt\right]}{\mathbb{E}\left[\int_T \mathbf{1}_{\{X(t) > u(t)\}} dt\right]} = \frac{\mathbb{E}[\mathcal{L}(\{t \in T : B(t, r) \subset E_X(u)\})]}{\mathbb{E}[\mathcal{L}(E_X(u) \cap T)]} \\ &= \frac{\mathbb{E}[\mathcal{L}(E_X(u)_{-r} \cap T)]}{\mathbb{E}[\mathcal{L}(E_X(u) \cap T)]}. \end{aligned}$$

□

Lemma 2. *Suppose that X and the corresponding threshold function u_p for some $p \in (0, 1)$ satisfy Assumption 1. Then Equation (1) holds with u_p in place of u for any compact $T \subset \mathbb{R}^2$ with positive Lebesgue measure, and any $r \geq 0$.*

Proof. The proof corresponds exactly with that of Proposition 1. □

Proof of Lemma 1. Let $r > 0$ and let $T \subset \mathbb{R}^2$ be compact with positive Lebesgue measure. Define $A := \{s \in \mathbb{R}^2 : \text{dist}(s, E_X(u)^c) = r\}$, and let $x \in A$. For each $\epsilon \in (0, r)$, the ball $B(x, \epsilon)$ contains an open ball \tilde{B} of radius $\epsilon/2$ such that for all $y \in \tilde{B}$, one has $\text{dist}(y, E_X(u)^c) < r$. In particular, $\tilde{B} \cap A = \emptyset$, and so the Lebesgue density of A at x cannot exceed $3/4$. By the Lebesgue differentiation theorem, the Lebesgue density of A at s is 1 for almost every $s \in A$. Since there are no elements of A for which this holds, $\mathcal{L}(A) = 0$.

Suppose the statement of the Lemma is false. Then, there exists an $r > 0$ such that $\mathbb{P}(\tilde{R}^{(u)}(0) = r \mid X(0) > u) > 0$, or equivalently, $\mathbb{P}(\tilde{R}^{(u)}(0) = r) > 0$. By stationarity and Fubini's theorem,

$$0 < \mathbb{P}(\tilde{R}^{(u)}(0) = r) = \mathbb{E}\left[\int_T \mathbf{1}_{\{\tilde{R}^{(u)}(s)=r\}} ds\right] = \mathbb{E}[\mathcal{L}(A)].$$

Hence, we have arrived at a contradiction, as $\mathbb{P}(\mathcal{L}(A) > 0) = 0$. □

The following lemmas are useful in the proof of Theorem 1 given below.

Lemma 3. *Let $A \subseteq \mathbb{R}^2$ and let $T \subset \mathbb{R}^2$ be compact, and let $r > 0$. The following identities hold.*

- $\mathcal{L}(A^c \cap T) = \mathcal{L}(T) - \mathcal{L}(A \cap T)$,
- $(A \cap T)_{-r} = A_{-r} \cap T_{-r} = ((A^c \cap T)_r)^c \cap T_{-r}$.

Proof. The first item holds by the additivity of the Lebesgue measure, and the two facts $(A^c \cap T) \cap (A \cap T) = \emptyset$ and $(A^c \cap T) \cup (A \cap T) = T$.

Now to prove the second item, note that $(S^c)_r = (S_{-r})^c$ for any set $S \subseteq \mathbb{R}^2$ (Cotsakis 2023, Lemma 1). Now, by De Morgan's laws,

$$\begin{aligned} ((A \cap T)_{-r})^c &= (A^c \cup T^c)_r = \bigcup_{x \in A^c \cup T^c} B(x, r) = \left(\bigcup_{x \in A^c} B(x, r) \right) \cup \left(\bigcup_{y \in T^c} B(y, r) \right) \\ &= (A^c)_r \cup (T^c)_r = (A_{-r})^c \cup (T_{-r})^c = (A_{-r} \cap T_{-r})^c. \end{aligned}$$

This proves the first equality by taking complements. For the second equality, write

$$((A^c \cap T)_r)^c \cap T_{-r} = (A \cup T^c)_{-r} \cap T_{-r} = ((A \cup T^c) \cap T)_{-r} = (A \cap T)_{-r}.$$

□

Lemma 4. *Let $T \subset \mathbb{R}^2$ be compact. It holds for $r > 0$ that*

$$\mathcal{L}(E_X(u) \cap T_{-r}) - \mathcal{L}((E_X(u) \cap T)_{-r}) \leq \frac{9\pi r}{4} \left(\ell(\partial E_X(u) \cap T) + N_T^{(u)} r \right), \quad (11)$$

where $N_T^{(u)}$ is as defined in Definition 4.

Proof. By Lemma 3, the LHS of Equation (11) is equal to the Lebesgue measure of $(E_X(u) \cap T_{-r}) \setminus E_X(u)_{-r}$. Remark that for $r > 0$,

$$(E_X(u) \cap T_{-r}) \setminus E_X(u)_{-r} \subseteq (\partial E_X(u))_r \cap T_{-r} \subseteq (\partial E_X(u) \cap T)_r.$$

By following the construction in (Cotsakis et al. 2023, Lemma 1), let $\gamma^{(i)}$ be the i^{th} connected component of $\partial E_X(u) \cap T$. It is possible to write

$$\gamma^{(i)} = \bigcup_{j=1}^{\lfloor \ell(\gamma^{(i)})/r \rfloor + 1} \beta^{(i,j)},$$

with $\ell(\beta^{(i,j)}) \leq r$ for $j \in \{1, \dots, \lfloor \ell(\gamma^{(i)})/r \rfloor + 1\}$. Now,

$$\partial E_X(u) \cap T = \bigcup_{i=1}^{N_T^{(u)}} \bigcup_{j=1}^{\lfloor \ell(\gamma^{(i)})/r \rfloor + 1} \beta^{(i,j)},$$

and so

$$(\partial E_X(u) \cap T)_r \subseteq \bigcup_{i=1}^{N_T^{(u)}} \bigcup_{j=1}^{\lfloor \ell(\gamma^{(i)})/r \rfloor + 1} \beta_r^{(i,j)}.$$

With the length of each $\beta^{(i,j)}$ is bounded by r , it follows that each $\beta_r^{(i,j)}$ is contained in a ball of radius $3r/2$. Therefore,

$$\begin{aligned} \mathcal{L}\left(\bigcup_{i=1}^{N_T^{(u)}} \bigcup_{j=1}^{\lfloor \ell(\gamma^{(i)})/r \rfloor + 1} \beta_r^{(i,j)}\right) &\leq \left(\frac{\ell(\partial E_X(u) \cap T)}{r} + N_T^{(u)}\right) \pi(3r/2)^2 \\ &= \frac{9\pi r}{4} \left(\ell(\partial E_X(u) \cap T) + N_T^{(u)} r\right). \end{aligned}$$

□

Proof of Theorem 1. Let $T \subset \mathbb{R}^2$ be a compact, convex set, and fix $r > 0$. By Lemma 3, for all $r > 0$,

$$\begin{aligned} \mathcal{L}((E_X(u) \cap T)_{-r}) &= \mathcal{L}(T_{-r}) - \mathcal{L}((E_X(u)^c \cap T)_r \cap T_{-r}) \\ &= \mathcal{L}(T_{-r}) - \mathcal{L}((E_X(u)^c \cap T)_r) + \mathcal{L}((\partial T)_r \cap A^{(r,T)}), \end{aligned}$$

for some $A^{(r,T)} \subset \mathbb{R}^2$. Now, $E_X(u)^c \cap T$ has positive reach almost surely, and for each positive r smaller than the reach of $E_X(u)^c \cap T$, there is a corresponding set $A^{(r,T)}$ such that

$$\begin{aligned} \mathcal{L}((E_X(u) \cap T)_{-r}) &= \mathcal{L}(T_{-r}) - \left(\mathcal{L}(E_X(u)^c \cap T) + \ell(\partial(E_X(u)^c \cap T))r + \chi(E_X(u)^c \cap T)\pi r^2\right) \\ &\quad + \mathcal{L}((\partial T)_r \cap A^{(r,T)}) \\ &= \mathcal{L}(T_{-r}) - \mathcal{L}(T) + \mathcal{L}(E_X(u) \cap T) - \mathcal{L}(E_X(u) \cap T_{-r}) + \mathcal{L}(E_X(u) \cap T_{-r}) \\ &\quad - \ell(\partial(E_X(u) \cap T))r - \chi(E_X(u)^c \cap T)\pi r^2 + \mathcal{L}((\partial T)_r \cap A^{(r,T)}), \end{aligned}$$

almost surely. Therefore,

$$\limsup_{r \rightarrow 0} \left| \frac{\mathcal{L}(E_X(u) \cap T_{-r}) - \mathcal{L}((E_X(u) \cap T)_{-r})}{r} - \ell(\partial(E_X(u) \cap T)) \right| \leq 2\ell(\partial T), \quad (12)$$

almost surely. Together, Assumption 1 and Lemma 4 verify the hypotheses of the reverse Fatou lemma applied to (12), and so one achieves

$$\limsup_{r \rightarrow 0} \left| \frac{\mathbb{E}[\mathcal{L}(E_X(u) \cap T_{-r})] - \mathbb{E}[\mathcal{L}((E_X(u) \cap T)_{-r})]}{r} - \mathbb{E}[\ell(\partial(E_X(u) \cap T))] \right| \leq 2\ell(\partial T),$$

and by Lemma 2,

$$\limsup_{r \rightarrow 0} \left| \frac{\mathbb{E}[\mathcal{L}(E_X(u) \cap T_{-r})] \mathbb{P}(R_0^{(u)} \leq r)}{\mathbb{E}[\mathcal{L}(E_X(u) \cap T)] r} - \frac{\mathbb{E}[\ell(\partial(E_X(u) \cap T))]}{\mathbb{E}[\mathcal{L}(E_X(u) \cap T)]} \right| \leq \frac{2\ell(\partial T)}{\mathcal{L}(T) \mathbb{P}(X(0) > u)},$$

by a division of $\mathbb{E}[\mathcal{L}(E_X(u) \cap T)]$. Recall that T is arbitrary and so can be taken arbitrarily large such that its perimeter length is negligible to its area. This implies

$$\lim_{T \nearrow \mathbb{R}^2} \lim_{r \rightarrow 0} \frac{\mathbb{E}[\mathcal{L}(E_X(u) \cap T_{-r})] \mathbb{P}(R_0^{(u)} \leq r)}{\mathbb{E}[\mathcal{L}(E_X(u) \cap T)] r} = \frac{2C_1^*(E_X(u))}{C_2^*(E_X(u))}. \quad (13)$$

The result holds since, for any T ,

$$\frac{\mathbb{E}[\mathcal{L}(E_X(u) \cap T_{-r})]}{\mathbb{E}[\mathcal{L}(E_X(u) \cap T)]} = \frac{\mathcal{L}(T_{-r})}{\mathcal{L}(T)} \xrightarrow{r \rightarrow 0} 1.$$

□

B.2 Proof of Proposition 2

In [Kac & Slepian \(1959\)](#), it is shown that for a one-dimensional centered Gaussian process $\{Y(t)\}_{t \in \mathbb{R}}$ having the stationary covariance function in (5), it holds that

$$u(Y(t/u) - u) \mid \{Y(0) = u, Y'(0) > 0\} \xrightarrow{u \rightarrow \infty} -\frac{\alpha}{2}t^2 + \xi_\alpha t,$$

where the convergence holds for the finite dimensional distributions of the process (in t), and ξ_α is some random variable that depends on α and the sense of the conditioning on the event $Y(0) = u$, but not on t . Therefore, $u(Y(t/u) - u) \mid Y(0) > u$ converges in the same sense to $-\frac{\alpha}{2}t^2 + \xi_1 t + \xi_2$, where ξ_1 and ξ_2 are random variables, and $\xi_2 > 0$ almost surely. Now, focusing on the two-dimensional random field X , we see that X evaluated on any one-dimensional affine linear subspace of \mathbb{R}^2 is a Gaussian process, and so the analysis in the preceding paragraph applies to these processes. Therefore, seen as a process in t ,

$$u(X(t/u) - u) \mid X(0) > u \xrightarrow{u \rightarrow \infty} -\frac{\alpha}{2}\|t\|^2 + \langle \tilde{\xi}_\alpha, t \rangle + \xi, \quad (14)$$

for some random vector $\tilde{\xi}_\alpha$ that depends on α but not on t , and for some almost surely positive random variable ξ . One can show that $\xi \sim \text{Exp}(1)$ independently of α and t .

Now,

$$\begin{aligned} uR_0^{(u)} &\stackrel{d}{=} \sup \left\{ r \in \mathbb{R}^+ : B(0, r/u) \subset E_X(u) \right\} \mid X(0) > u \\ &\stackrel{d}{=} \sup \left\{ r \in \mathbb{R}^+ : B(0, r) \subset uE_X(u) \right\} \mid X(0) > u \\ &\stackrel{d}{=} \sup \left\{ r \in \mathbb{R}^+ : B(0, r) \subset E_{X(\cdot/u)}(u) \right\} \mid X(0) > u. \end{aligned}$$

Equation (14) implies that $E_{X(\cdot/u)}(u) \mid X(0) > u$ converges to a random disk containing the origin as $u \rightarrow \infty$, which finishes the proof.

□

B.3 Proofs and definitions for §4.1.2

Definition 10 (Definition 4 in [Dombry & Ribatet \(2015\)](#)). *The random field $W : \Omega \times T \rightarrow \mathbb{R}$ is an ℓ -Pareto random field with exponent $\alpha \in \mathbb{R}^+$ and spectral measure σ_ℓ if*

- $\mathbb{P}(W \in \mathcal{C}_0) = 1$,
- $\mathbb{P}(\ell(W) > u) = u^{-\alpha}$, for all $u > 1$,
- $W/\ell(W)$ and $\ell(W)$ are independent, and
- $\sigma_\ell(A) = \mathbb{P}(W/\ell(W) \in A)$ for $A \in \mathcal{B}(\mathcal{C}_0)$.

In this case, we write $W \sim P_{\alpha, \sigma_\ell}^\ell$

The link between regularly varying random fields and ℓ -Pareto random fields is made by the following lemma.

Lemma 5 (Theorem 3 in [Dombry & Ribatet \(2015\)](#)). *Let $X|_T \in \text{RV}_{\alpha, \sigma}(\mathcal{C}_0)$ with exponent $\alpha > 0$ and spectral measure σ on \mathcal{S} . Let $\ell : \mathcal{C}_0 \rightarrow [0, \infty)$ be a homogeneous cost functional that is continuous at the origin, and is nonzero on a subset of \mathcal{S} with positive σ measure. Let $W \sim P_{\alpha, \sigma_\ell}^\ell$ where*

$$\sigma_\ell(A) := \frac{1}{c} \int_{\mathcal{S}} \ell(x)^\alpha \mathbf{1}_{\{x/\ell(x) \in A\}} \sigma(dx), \quad A \in \mathcal{B}(\mathcal{C}_0),$$

with $c := \int_{\mathcal{S}} \ell(x)^\alpha \sigma(dx)$. Then,

$$\mathbb{P}(u^{-1}X|_T \in A \mid \ell(X|_T) > u) \xrightarrow{u \rightarrow \infty} \mathbb{P}(W \in A), \quad A \in \mathcal{B}(\mathcal{C}_0).$$

Proof of Proposition 3. We begin by showing the second equality in (6). By the continuity of X , the excursion set $E_X(u)$ is open, and so the events $\{\tilde{R}_0^{(u)} > r\}$ and $\{B(0, r) \subset E_X(u)\}$ are equal. Also, $E_X(u) = E_{X/u}(1)$, and so for $r < r_T$,

$$\begin{aligned} \mathbb{P}(R_0^{(u)} > r) &= \mathbb{P}(B(0, r) \subset E_X(u) \mid X(0) > u) = \mathbb{P}(B(0, r) \subset E_{X/u}(1) \mid X(0) > u) \quad (15) \\ &\xrightarrow{u \rightarrow \infty} \mathbb{P}(B(0, r) \subset E_{Y_0}(1)) = 1 - \mathbb{P}(\exists t \in B(0, r) : Y_0(t) \leq 1). \end{aligned}$$

The convergence in (15) holds by Lemma 5. To show the first equality in (6), remark that $(E_{Y_T}(u) \cap T)_{-r} = E_{Y_T}(u)_{-r} \cap T_{-r}$. Also, recall from Proposition 1 that

$$\begin{aligned} \mathbb{P}(R_0^{(u)} > r) &= \frac{\mathbb{E}[\mathcal{L}(E_X(u)_{-r} \cap T_{-r})]}{\mathbb{E}[\mathcal{L}(E_X(u) \cap T_{-r})]} = \frac{\mathbb{E}[\mathcal{L}((E_{X/u}(1) \cap T)_{-r}) \mid \|X\|_T > u]}{\mathbb{E}[\mathcal{L}(E_{X/u}(1) \cap T_{-r}) \mid \|X\|_T > u]} \\ &\xrightarrow{u \rightarrow \infty} \frac{\mathbb{E}[\mathcal{L}((E_{Y_T}(1) \cap T)_{-r})]}{\mathbb{E}[\mathcal{L}(E_{Y_T}(1) \cap T_{-r})]} = \frac{\mathbb{E}[\mathcal{L}((E_{Y_T}(1) \cap T)_{-r})]}{\mathcal{L}(T_{-r})\mathbb{P}(Y_T(0) > 1)}. \end{aligned}$$

□

B.4 Proof of Propostion 6

We start by decomposing

$$\widehat{\theta}_s^{(n)}(p_0, p_n) = \frac{A_n - B_n}{C - D_n},$$

where

$$\begin{aligned} A_n &= \log(\widehat{q_{50\%}}^{(n)}(R_s^{(u_{pn})})), & B_n &= \log(\widehat{q_{50\%}}^{(n)}(R_s^{(u_{p_0})})) \\ C &= \log(-\log(1 - p_0)), & D_n &= \log(-\log(1 - p_n)). \end{aligned}$$

We begin by showing

$$-\frac{A_n}{D_n} \xrightarrow[n \rightarrow \infty]{\mathbb{P}} \theta_s. \quad (16)$$

Under Assumption 2, for any $\alpha \in (0, 1)$, the function $h_\alpha(x) := q_\alpha(R_s^{(u_{p(x)})})$ with $x > 0$ and $p(x) = 1 - e^{-x}$ is regularly varying with index $-\theta_s$. Thus, by the Karamata characterization theorem, $x^{\theta_s} h_\alpha(x)$ is slowly varying. For $\epsilon > 0$, and $\alpha \in (0, 1)$, there exists $x_{\alpha, \epsilon} \in \mathbb{R}^+$ such that

$$-\epsilon \log x < \theta_s \log x + \log h_\alpha(x) < \epsilon \log x,$$

for all $x > x_{\alpha, \epsilon}$. Equivalently,

$$\frac{\log h_\alpha(x)}{\log x} \in (-\theta_s - \epsilon, -\theta_s + \epsilon),$$

for all $x > x_{\alpha, \epsilon}$. Let $n \in \mathbb{N}$, and let \mathcal{A}_n denote the event $\{\widetilde{R}_i^{(u_{pn})}(s) > 0, \text{ for at least one } i = 1, \dots, n\}$. By the assumption that $n(1 - p_n) \rightarrow \infty$ as $n \rightarrow \infty$, we have $\mathbb{P}(\mathcal{A}_n) \rightarrow 1$. Choose $\underline{\alpha} \in (0, 1/2)$ and $\bar{\alpha} \in (1/2, 1)$. Notice that for $x = -\log(1 - p_n) = \exp(D_n)$, one has $p(x) = p_n$, and

$$\begin{aligned} \bar{\alpha} - \underline{\alpha} &= \mathbb{P}(h_{\underline{\alpha}}(x) < R_s^{(u_{pn})} < h_{\bar{\alpha}}(x)) \\ &\leq \mathbb{P}(h_{\underline{\alpha}}(x) < \widehat{q_{50\%}}^{(n)}(R_s^{(u_{pn})}) < h_{\bar{\alpha}}(x) \mid \mathcal{A}_n) \\ &\leq \frac{\mathbb{P}(h_{\underline{\alpha}}(x) < \widehat{q_{50\%}}^{(n)}(R_s^{(u_{pn})}) < h_{\bar{\alpha}}(x))}{\mathbb{P}(\mathcal{A}_n)} \\ &= \frac{\mathbb{P}\left(\frac{\log h_{\underline{\alpha}}(x)}{\log(x)} < \frac{A_n}{D_n} < \frac{\log h_{\bar{\alpha}}(x)}{\log(x)}\right)}{\mathbb{P}(\mathcal{A}_n)}. \end{aligned}$$

As seen previously, for n (or equivalently x) large enough, one has

$$\mathbb{P}\left(\frac{\log h_{\underline{\alpha}}(x)}{\log(x)} < \frac{A_n}{D_n} < \frac{\log h_{\bar{\alpha}}(x)}{\log(x)}\right) \leq \mathbb{P}\left(\frac{A_n}{D_n} \in (-\theta_s - \epsilon, -\theta_s + \epsilon)\right).$$

The left-hand side is bounded below by $\mathbb{P}(\mathcal{A}_n)(\bar{\alpha} - \underline{\alpha})$ which can be made arbitrarily close to 1 by choice of $\bar{\alpha}$, $\underline{\alpha}$, and n . This proves (16).

Since $D_n \rightarrow \infty$ as $n \rightarrow \infty$, the statement of the proposition holds since B_n converges to a constant $\log(q_{50\%}(R_s^{(u_{p_0})}))$ in probability as $n \rightarrow \infty$. \square

References

- Adler, R. J. & Taylor, J. E. (2007), *Random fields and geometry*, Springer Monographs in Mathematics, Springer, New York.
- AghaKouchak, A., Chiang, F., Huning, L. S., Love, C. A., Mallakpour, I., Mazdidasni, O., Moftakhari, H., Papalexiou, S. M., Ragno, E. & Sadegh, M. (2020), ‘Climate extremes and compound hazards in a warming world’, *Annual Review of Earth and Planetary Sciences* **48**, 519–548.
- Beliaev, D., McAuley, M. & Muirhead, S. (2020), ‘On the number of excursion sets of planar Gaussian fields’, *Probability Theory and Related Fields* **178**(3), 655–698.
- Berman, S. (1971), ‘Excursions above high levels for stationary Gaussian processes’, *Pacific Journal of Mathematics* **36**(1), 63–79.
- Berman, S. M. (1982), ‘Sojourns and Extremes of Stationary Processes’, *The Annals of Probability* **10**(1), 1–46.
- Biermé, H., Di Bernardino, E., Duval, C. & Estrade, A. (2019), ‘Lipschitz-Killing curvatures of excursion sets for two-dimensional random fields’, *Electronic Journal of Statistics* **13**(1), 536–581.
- Bleau, A. & Leon, L. J. (2000), ‘Watershed-based segmentation and region merging’, *Computer Vision and Image Understanding* **77**(3), 317–370.
- Bolin, D. & Lindgren, F. (2015), ‘Excursion and contour uncertainty regions for latent Gaussian models’, *Journal of the Royal Statistical Society: Series B (Statistical Methodology)* **77**(1), 85–106.
- Cambanis, S. (1973), ‘On some continuity and differentiability properties of paths of gaussian processes’, *Journal of Multivariate Analysis* **3**(4), 420–434.
- Coles, S., Heffernan, J. & Tawn, J. (1999), ‘Dependence measures for extreme value analyses’, *Extremes* **2**, 339–365.
- Cotsakis, R. (2023), ‘Computable bounds for the reach and r-convexity of subsets of \mathbb{R}^d ’, Preprint [arXiv:2212.01013](https://arxiv.org/abs/2212.01013).
- Cotsakis, R., Di Bernardino, E. & Duval, C. (2022), ‘Surface area and volume of excursion sets observed on point cloud based polytopic tessellations’, Preprint [arXiv:2209.10383](https://arxiv.org/abs/2209.10383).
- Cotsakis, R., Di Bernardino, E. & Opitz, T. (2023), ‘On the perimeter estimation of pixelated excursion sets of two-dimensional anisotropic random fields’, *Scandinavian Journal of Statistics*.

- Dalmao, F., León, J. R., Mordecki, E. & Mourareau, S. (2019), ‘Asymptotic normality of high level-large time crossings of a Gaussian process’, *Stochastic Processes and their Applications* **129**(4), 1349–1370.
- de Fondeville, R. & Davison, A. C. (2022), ‘Functional peaks-over-threshold analysis’, *Journal of the Royal Statistical Society Series B: Statistical Methodology* **84**(4), 1392–1422.
- de Haan, L. & Ferreira, A. (2006), *Extreme value theory: an introduction*, Vol. 21, Springer.
- Di Bernardino, E., Estrade, A. & Opitz, T. (2022), ‘Spatial extremes and stochastic geometry for Gaussian-based peaks-over-threshold processes’, *Preprint [hal-03825701](https://hal.archives-ouvertes.fr/hal-03825701)* .
- Dombry, C. & Ribatet, M. (2015), ‘Functional regular variations, Pareto processes and peaks over threshold’, *Statistics and Its Interface* **8**, 9–17.
- Dombry, C., Ribatet, M. & Stoev, S. (2018), ‘Probabilities of Concurrent Extremes’, *Journal of the American Statistical Association* **113**(524), 1565–1582.
- Federer, H. (1959), ‘Curvature measures’, *Transactions of the American Mathematical Society* **93**(3), 418–491.
- Ferreira, A. & de Haan, L. (2014), ‘The generalized Pareto process; with a view towards application and simulation’, *Bernoulli* **20**(4), 1717–1737.
- Friedman, A. (2007), *Advanced Calculus*, Dover Books on Mathematics, Dover Publications.
- Gordon, R. D. (1941), ‘Values of Mills' Ratio of Area to Bounding Ordinate and of the Normal Probability Integral for Large Values of the Argument’, *The Annals of Mathematical Statistics* **12**(3), 364–366.
- Heffernan, J. E. & Tawn, J. A. (2004), ‘A conditional approach for multivariate extreme values (with discussion)’, *Journal of the Royal Statistical Society: Series B (Statistical Methodology)* **66**(3), 497–546.
- Huser, R., Opitz, T. & Thibaud, E. (2017), ‘Bridging asymptotic independence and dependence in spatial extremes using Gaussian scale mixtures’, *Spatial Statistics* **21**, 166–186.
- Huser, R. & Wadsworth, J. L. (2022), ‘Advances in statistical modeling of spatial extremes’, *Wiley Interdisciplinary Reviews: Computational Statistics* **14**(1), e1537.
- Kac, M. & Slepian, D. (1959), ‘Large Excursions of Gaussian Processes’, *The Annals of Mathematical Statistics* **30**(4), 1215–1228.

- Kratz, M. F. (2006), ‘Level crossings and other level functionals of stationary Gaussian processes’, *Probability Surveys* **3**, 230–288.
- Leadbetter, M. R., Lindgren, G. & Rootzén, H. (1983), *Extremes and Related Properties of Random Sequences and Processes*, Springer New York.
- Moloney, N. R., Faranda, D. & Sato, Y. (2019), ‘An overview of the extremal index’, *Chaos: An Interdisciplinary Journal of Nonlinear Science* **29**(2), 022101.
- Perkins, S., Alexander, L. & Nairn, J. (2012), ‘Increasing frequency, intensity and duration of observed global heatwaves and warm spells’, *Geophysical Research Letters* **39**(20).
- Pham, V.-H. (2013), ‘On the rate of convergence for central limit theorems of sojourn times of Gaussian fields’, *Stochastic Processes and their Applications* **123**(6), 427–464.
- Ripley, B. (1988), *Statistical Inference for Spatial Processes*, Cambridge University Press.
- Rosenblatt, M. (1956), ‘A Central Limit Theorem and a Strong Mixing Condition’, *Proceedings of the National Academy of Sciences of the United States of America* **42**(1), 43–47.
- Schneider, R. & Weil, W. (2008), *Stochastic and Integral Geometry*, Springer, Berlin, Heidelberg.
- Serra, J. (1984), *Image Analysis and Mathematical Morphology*, Academic Press.
- Sethian, J. A. (1996), ‘A fast marching level set method for monotonically advancing fronts’, *Proceedings of the National Academy of Sciences* **93**(4), 1591–1595.
- Sezgin, M. & Sankur, B. I. (2004), ‘Survey over image thresholding techniques and quantitative performance evaluation’, *Journal of Electronic imaging* **13**(1), 146–168.
- Silva, F. & Steele, J. (2014), ‘New methods for reconstructing geographical effects on dispersal rates and routes from large-scale radiocarbon databases’, *Journal of Archaeological Science* **52**, 609–620.
- Simpson, E. S., Opitz, T. & Wadsworth, J. L. (2023), ‘High-dimensional modeling of spatial and spatio-temporal conditional extremes using INLA and Gaussian Markov random fields’, *Extremes* pp. 1–45.
- Sommerfeld, M., Sain, S. & Schwartzman, A. (2018), ‘Confidence regions for spatial excursion sets from repeated random field observations, with an application to climate’, *Journal of the American Statistical Association* **113**(523), 1327–1340.
- Tawn, J., Shooter, R., Towe, R. & Lamb, R. (2018), ‘Modelling spatial extreme events with environmental applications’, *Spatial statistics* **28**, 39–58.

- Thäle, C. (2008), ‘50 years sets with positive reach—a survey’, *Surveys in Mathematics and its Applications* **3**, 123–165.
- Thibaud, E. & Opitz, T. (2015), ‘Efficient inference and simulation for elliptical Pareto processes’, *Biometrika* **102**(4), 855–870.
- Vidal, J.-P., Martin, E., Franchistéguy, L., Baillon, M. & Soubeyroux, J.-M. (2010), ‘A 50-year high-resolution atmospheric reanalysis over france with the safran system’, *International journal of climatology* **30**(11), 1627–1644.
- Wadsworth, J. L. & Tawn, J. A. (2022), ‘Higher-dimensional spatial extremes via single-site conditioning’, *Spatial Statistics* **51**, 100677.
- Wood, S. N. (2017), *Generalized additive models: an introduction with R*, CRC press.
- Zhang, Z., Huser, R., Opitz, T. & Wadsworth, J. (2022), ‘Modeling spatial extremes using normal mean-variance mixtures’, *Extremes* **25**(2), 175–197.